ENGINEERING EXPERIMENT STATION

Georgia Institute of Technology

PROJECT INITIATION

Date 10-19-59

PROJECT TITLE: Countermeasures Research for Advanced Air Force Strategic Vehicles

PROJECT NO: A-438

PROJECT DIRECTOR: Fred Dixon

SPONSOR: Dept. of the Air Force, Wright Air Development Center

EFFECTIVE: 2-1-59 * ESTIMATED TO RUN UNTIL: 12-31-59

TYPE AGREEMENT: Contract No. AF 33(616)-6292

Amount: $130,000.00

Reports: Monthly Progress Reports
Quarterly Technical Documentary Notes
Final Technical Documentary Report
Charts and Slides

Contact Person: Commander
Wright Air Development Center
Wright-Patterson AFB, Ohio
Attn:WCKSC(for administrative matters)
WCLG (for technical matters

*Anticipatory Costs in an amount not to exceed $8,000 allowed from 1-1-59 to 1-31-59

Assigned to Defense Branch, Physical Sciences Divsion

Copies to:

- ☐ Project Director
- ☐ Director
- ☐ Associate Director
- ☐ Assistant Director(s)
- ☐ Division Chiefs
- ☐ Branch Head
- ☐ Accounting
- ☐ General Office Services
- ☐ Rich Electronic Computer Center
- ☐ Purchasing
- ☐ Engineering Design Services
- ☐ Technical Information Section
- ☐ Photographic Laboratory
- ☐ Shop
- ☐ Security Officer
- ☐ Report Section
- ☐ Library

_____

ES FORM 400 (Rev 7-59)

Design Criteria
For
Pellet-Dispersing Warheads

Gilbert C. Knollman
and
Joseph J. Moder

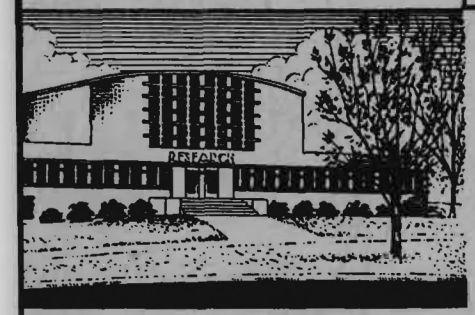

Engineering Experiment Station
Georgia Institute of Technology
Atlanta, Georgia

DESIGN CRITERIA FOR PELLET-DISPERSING WARHEADS*

Gilbert C. Knollman and Joseph J. Moder

Engineering Experiment Station
Georgia Institute of Technology
Atlanta, Georgia

A warhead is presumed to be so designed as to provide a radial dispersion of small pellets without significantly altering their collective forward motion. Thus, at the moment of target interception, the pellets are taken as randomly distributed over either a circular or an elliptical lamina, and those paraboloidal and uniform distributions which lead to optimum target kill probabilities are derived. Design criteria are noted which tend to yield the largest overall kill probability. Target and lamina size, individual pellet mass, overall mass, kill probability of a single pellet which hits the target, and the random errors of predicting target position and of placing the pellet array at that position are all taken into account. Errors in improper orientation of the pellet lamina are neglected. An assessment is made of the basic proposition that the kill probability of every pellet striking the target is the same, independent of the number of previous hits; thereby some "limits of applicability" are established for the present study. In conclusion, an application of the mathematical results to a shotgun-bird system is presented.

1. Introduction

A comprehensive study has been made of a target-weapon system in three-dimensional space in which the weapon is a two-dimensional array of small pellets that will cause significant physical damage to the target upon impact. The pellets are assumed to be randomly distributed throughout a circular or elliptical lamina according to a specified "law of distribution" at the moment of interception. Emphasis has been placed on the determination of kill probabilities for various forms of spatial distribution of

*Based on research supported in part under contract number AF 33(616)-6292. To be presented at the Eighteenth National Meeting of the Operations Research Society of America, Detroit, Michigan, October 10-12, 1960.

pellets throughout the laminas, with account taken of such factors as target size, overall pattern size, individual pellet mass, overall mass, and the kill probability of a single pellet which hits the target. The analysis includes the possibility of two error sources — namely, probable errors of predicting target position and of placing the pellet pattern at that target position.*

At the time the target center is overtaken by the pellet array and lies within the pellet-pattern plane, the projected target area in this plane is conveniently represented by that of a circle of radius $\underline{r}_T$ (called the effective target circle), while the pellet pattern has an overall cross-sectional radius $\underline{r}_P$ (in the circular lamina case) or semiaxis lengths $\underline{a}_P$ and $\underline{b}_P$ (in the elliptical lamina case). It is assumed that $\underline{r}_T$ is much smaller than the smallest diameter of the pellet pattern so that the actual geometric shape of the target is relatively unimportant. However, $\underline{r}_T$ is not considered as small compared to the spacing between individual pellets in the laminar pattern.

Figure 1 illustrates three forms of pellet distributions which are treated in the present analysis. Since it will be shown that the ideal distribution is paraboloidal in form, the paraboloid which yields overall the largest kill probability (labeled "optimum paraboloid" in Figure 1) is investigated initially for both the circular and the elliptical laminas. Next, that uniform distribution which gives the highest kill probability (labeled "optimum cylinder") is treated for both patterns to compare with the optimum paraboloid. Lastly, that paraboloid of revolution giving the largest kill probability (designated "optimum paraboloid of revolution") is included (for the circular lamina) to allow for comparisons between symmetric and asymmetric paraboloidal distributions.

Maximum Kill Probability in each of the cases shown in Figure 1 occurs for specific values of the pattern radius or semiaxis lengths. These maxima are computed and plotted versus a dimensionless parameter involving the effective radius of the target circle, individual pellet mass, overall mass, kill probability of a single pellet, and the error variances. Values are

*A general class of problems involving the combination of two random errors is discussed by Grad and Solomon [1].

given for the lamina radius or semiminor axis length which corresponds to the maximum Kill Probability. In addition, graphs are presented of Kill Probability versus pattern radius or semiminor axis length to illustrate the destruction probability for "early" or "late" arrival of the pellet array at the target position. Following the mathematical presentation, there appear a summary of the basic results and indications of some desirable design characteristics to incorporate in pellet-dispersing warheads. Finally, an application of the theory is made to a shotgun-bird system.

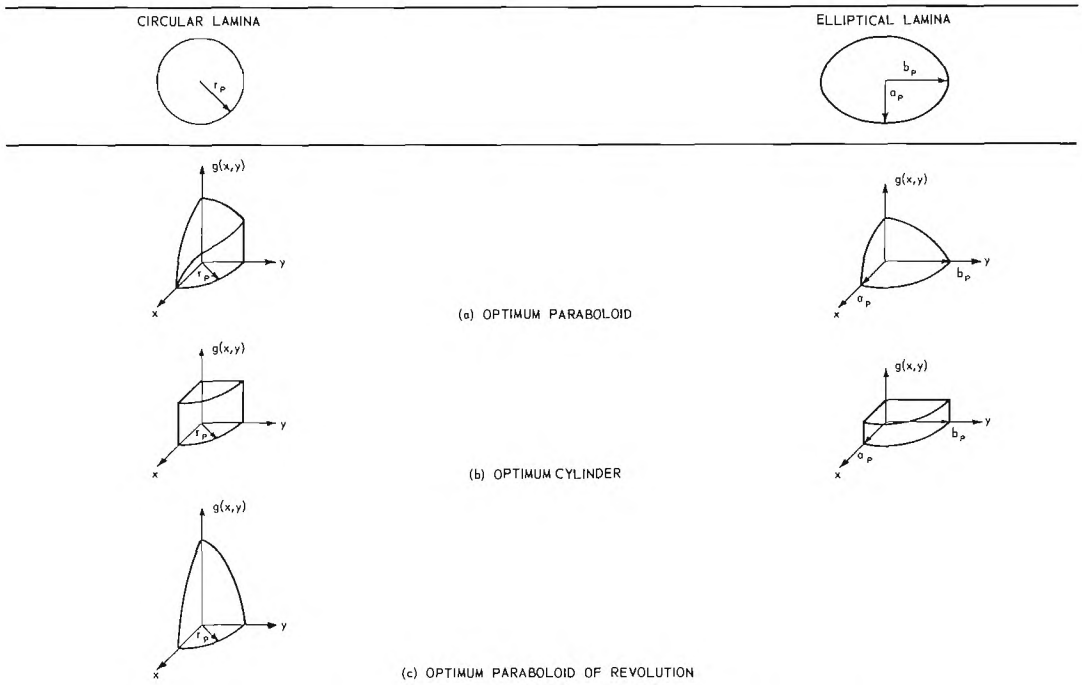

Figure 1. Illustrating Paraboloidal and Cylindrical Pellet Distributions Which Yield Categorically Optimum Kill Probabilities.

A basic assumption throughout is that the probability of destroying the target with any hit by a pellet is always the same, irrespective of the number of previous hits. This means that a pellet will only destroy the target if it hits a "vital spot," a hypothesis stated by Morse and Kimball [2] to be adequate in cases such as torpedoes against cargo ships and AA shells against aircraft. An assessment of the independent probability assumption is made in Section 10 to establish some "limits of applicability" for the present study.

2. Problem Geometry

At the instant of interception, the effective target circle coincides with the plane of the laminar pellet pattern, but the distance between centers of the target circle and the pellet pattern is typically nonzero. Figure 2 depicts two representative cases: one in which the target circle lies within the bounds of the pellet lamina, so that a kill is possible; the other in which no interception occurs, making destruction an impossibility. The pellet pattern is depicted as an elliptical lamina; the circular lamina case shown

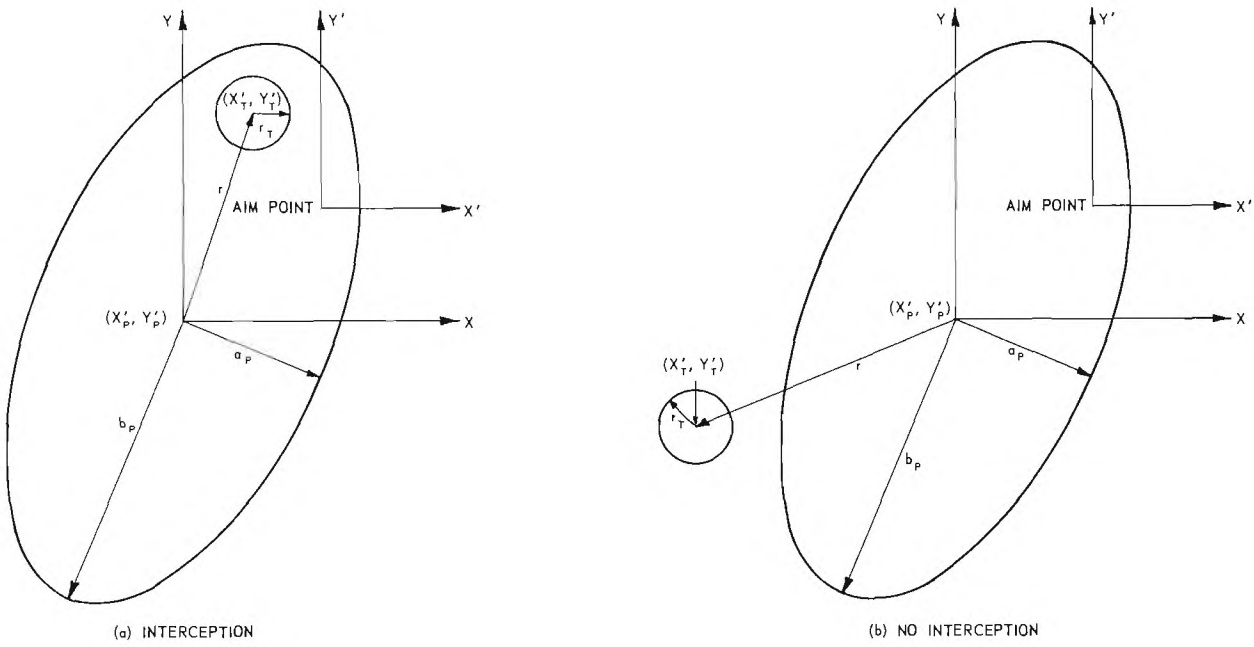

Figure 2. Typical Relative Positions of Effective Target Circle and Pellet Lamina Within the Plane of Interception.

in Figure 1 is, of course, the special case of an elliptical lamina with equal axis lengths. As noted earlier, r_T is assumed very much less than a_P, but has been exaggerated in Figure 2 for illustrative purposes.*

The Cartesian reference frame X′, Y′ is defined in the plane of interception with origin at the point of aim and with the Y′-axis drawn vertically upward. The coordinates X'_P and Y'_P, which locate the center of the pellet

*Contrary to conventional notation, the semiminor and semimajor axis lengths of the pellet lamina are represented by a_P and b_P, respectively.

pattern relative to this frame, may be regarded as the "lateral" and "vertical" errors incurred in attempting to place the center of the pellet array at the predicted target position. Similarly, lateral and vertical errors in predicted target position are represented by the coordinates $\underline{X}_T'$ and $\underline{Y}_T'$. These errors combine to give a net "miss distance" $\underline{r}$ between actual pellet pattern and target centers which can be written as

$$(1a) \qquad r = (X^2 + Y^2)^{\frac{1}{2}} \ ,$$

where $X = (X_T' - X_P')$ and $Y = (Y_T' - Y_P')$ are new coordinates locating the actual target center relative to a translated reference frame with origin at the center of the pellet pattern.

We assume that the coordinate pairs (X_T', Y_T') and (X_P', Y_P') each have a bivariate normal distribution with zero mean -- the associated variances and covariances being designated $\underline{\sigma}^2_{X_T'}$, $\underline{\sigma}^2_{Y_T'}$, $\underline{\sigma}^2_{X_P'}$, $\underline{\sigma}^2_{Y_P'}$, $\underline{\sigma}_{X_T'Y_T'}$ and $\underline{\sigma}_{X_P'Y_P'}$. Then $\underline{X}$ and $\underline{Y}$ also have a bivariate normal distribution with mean zero, whose variances and covariance are given by

$$(1b) \qquad \sigma_X^2 = \sigma^2_{X_T'} + \sigma^2_{X_P'} \ ,$$

$$(1c) \qquad \sigma_Y^2 = \sigma^2_{Y_T'} + \sigma^2_{Y_P'} \ ,$$

$$(1d) \qquad \sigma_{XY} = \sigma_{X_T'Y_T'} + \sigma_{X_P'Y_P'} \ .$$

A third orthogonal coordinate system x,y is now introduced in the plane of interception. This reference frame has the same origin as the X,Y system but is rotated counterclockwise therefrom by an angle $\underline{\varphi}$. The coordinates (x,y) of the actual target center in this system are assumed to have a bivariate normal distribution with mean zero. Equation (1a) for the miss distance $\underline{r}$ is written in terms of these coordinates as

$$(2a) \qquad r = (x^2 + y^2)^{\frac{1}{2}} \ .$$

The angle $\underline{\varphi}$ can always be chosen to align the axes of the x,y frame with those of the composite error ellipse so that the covariance $\underline{\sigma}_{xy}$ (of $\underline{x}$ and $\underline{y}$)

is zero, and the variances are

$$\sigma_x^2 = \frac{1}{2}\{(\sigma_X^2 + \sigma_Y^2) - [(\sigma_X^2 - \sigma_Y^2)^2 + 4\,\sigma_{XY}^2]^{\frac{1}{2}}\} \quad , \tag{2b}$$

$$\sigma_y^2 = \frac{1}{2}\{(\sigma_X^2 + \sigma_Y^2) + [(\sigma_X^2 - \sigma_Y^2)^2 + 4\,\sigma_{XY}^2]^{\frac{1}{2}}\} \quad . \tag{2c}$$

This process of diagonalizing the covariance matrix is discussed in Appendix A, where Equations (2b) and (2c) and also the requisite angle φ are derived.

The subsequent mathematical development is formulated with reference to the x,y coordinate system, wherein the ellipse of composite error variance is in standard position. Generally, the axes of the elliptical pellet pattern will not coincide with those of the x,y system due to errors incurred in attempting to properly orient the pellet lamina. However, to avoid unreasonable complications in the ensuing analysis, it is assumed that the elliptical pellet lamina is also in standard position in the x,y frame, and further that its major axis coincides with that of the error ellipse.

3. Computation of Intercept Probability

The term "Intercept Probability" as used here means the probability that the effective target circle and the pellet pattern will overlap somewhere in the plane of interception (see Figure 2a).* Insofar as the radius r_T of the effective target circle can be considered small compared to the smallest pellet pattern dimension a_P, a practical criterion for an Intercept is the condition that the center of the target circle lie within the boundary of the pellet pattern. Expressed mathematically, the Intercept Probability is

$$P\{\text{Intercept}\} = \frac{2}{\pi\,\sigma_x\sigma_y}\int_0^{a_P}\int_0^{\frac{b_P}{a_P}(a_P^2 - x^2)^{\frac{1}{2}}} \exp\left[-\frac{1}{2}\left(\frac{x^2}{\sigma_x^2} + \frac{y^2}{\sigma_y^2}\right)\right] dy\,dx \quad , \tag{3a}$$

where b_P and a_P are the semimajor and semiminor axis lengths of the pattern ellipse, respectively, and σ_x and σ_y are defined in (2b) and (2c). In polar-coordinate notation the above equation takes the form

---

*Since the pellets are random in their distribution within the pattern, an "intercept" of the target by the pellet array does not necessarily constitute a "hit."

$$(3b) \qquad P\{\text{Intercept}\} = \frac{1}{2\pi\,\sigma_x\sigma_y}\int_0^{2\pi}\int_0^{r^+} \exp\left[-\frac{r^2}{2}\left(\frac{\cos^2\theta}{\sigma_x^2}+\frac{\sin^2\theta}{\sigma_y^2}\right)\right] r\,dr\,d\theta \quad ,$$

where

$$(3c) \qquad r^+ = a_P\,b_P\,(b_P^2\cos^2\theta + a_P^2\sin^2\theta)^{-\frac{1}{2}} \quad .$$

Some simplification is gained in subsequent mathematical procedures by normalizing "length" quantities with respect to the standard deviations. Thus, the following substitutions are made in (3b):

$$(4a) \qquad \rho_a = \frac{a_P}{(\sigma_x\sigma_y)^{\frac{1}{2}}} \quad ,$$

the normalized semiminor axis length of the pellet pattern ellipse, and

$$(4b) \qquad \rho_b = \frac{b_P}{(\sigma_x\sigma_y)^{\frac{1}{2}}} \quad ,$$

the normalized semimajor axis length. In addition, the ratio of error standard deviations is represented by

$$(5a) \qquad \beta = \frac{\sigma_x}{\sigma_y} \leq 1 \quad ,$$

where σ_x and σ_y are arbitrarily chosen so that $\sigma_x \leq \sigma_y$, and the ratio of pellet-pattern axes by

$$(5b) \qquad K = \frac{a_P}{b_P} = \frac{\rho_a}{\rho_b} \leq 1 \quad .$$

Upon introduction of the substitution

$$(6) \qquad w = \frac{r^2}{\sigma_x\sigma_y}$$

in conjunction with Equations (4) and (5), one then obtains for the Intercept Probability

$$(7a) \qquad P\{\text{Intercept}\} = \int_0^{2\pi}\int_0^{w^+} \frac{1}{4\pi}\exp\left[-\frac{w}{2\beta}(\cos^2\theta + \beta^2\sin^2\theta)\right] dw\,d\theta \quad ,$$

where

$$(7b) \qquad w^+ = \rho_a^2\,(\cos^2\theta + K^2\sin^2\theta)^{-1} \quad .$$

4. Computation of Kill Probability

The term "Kill Probability" (meaning the probability of target destruction or disablement) implies not only that the target will lie within the pellet-pattern area at the time of interception but that it actually will be hit by one or more of the pellets, to each of which is ascribed a certain chance of striking some vital point in the target. The determination of Kill Probability therefore involves three factors: the likelihood of finding the target center within an interval dr at any given distance r from the center of the pellet pattern, the number of pellets likely to be encompassed at that distance by the effective target circle, and the probability of target disablement associated with each pellet hit.

The first of these factors is the differential Intercept Probability, given in normalized form by $f(w,\theta)\ dw\ d\theta$, where $f(w,\theta)$ denotes the normalized probability density function of the miss distance r and is the integrand in Equation (7a). The second and third factors will be considered in combination as a single "effectiveness function"—designated $h(w,\theta)$—which represents the conditional probability of a Kill, given that an Intercept has occurred at normalized distance $\sqrt{w}$. Then the Kill Probability is written

$$P\{\text{Kill}\} = \int_0^{2\pi} \int_0^{w^\dagger} h(w,\theta)\ f(w,\theta)\ dw\ d\theta \quad , \tag{8}$$

where the integration extends over the entire area wherein pellets exist. Thus, the total Kill Probability is given in terms of an "extrinsic" function $f(w,\theta)$, which contributes the effect of random errors in predicted target position and actual weapon placement, and an "intrinsic" function $h(w,\theta)$ which takes into account such things as distribution of pellets within the laminar pattern, the effective target area, and the vulnerability of the target to hits from pellets of given mass.

With the differential Kill Probability written as

$$dP\{\text{Kill}\} = P\{\text{Kill}\,|\,\text{Intercept}\}\ dP\{\text{Intercept}\} \quad , \tag{9}$$

reference to Equation (8) reveals that the normalized effectiveness function $h(w,\theta)$ may be regarded as the probability that a kill occurs given that an intercept has taken place. If every pellet within the pellet lamina has the

same mass m and if the total mass involved is M, then there will be M/m individual pellets distributed throughout the pattern. Assuming that the total number of pellets (M/m) will be very large while the ratio of target size to pellet-pattern size (r_T/a_P) is very small, and defining the normalized average or expected number of pellet hits occurring in the event of an Intercept to be $g(w,\theta)$, one may express the actual number of pellets hitting the target by the Poisson distribution function.* Hence, the probability that exactly i pellets will hit the target, provided an Intercept occurs, is

$$P\{i \text{ Hits} | \text{Intercept}\} = \frac{g^i e^{-g}}{i!} , \quad i = 0, 1, 2, \ldots . \tag{10}$$

To conserve the pellet number, $g(w,\theta)$ must satisfy the following integral equation:

$$\int_0^{2\pi} \int_0^{r^+} \frac{g(w,\theta)}{\pi r_T^2} \, r \, dr \, d\theta = \frac{M}{m} . \tag{11}$$

With the introduction of Equations (5), (6), and (7b) and the normalizing conditions (4), Equation (11) reduces to

$$\int_0^{2\pi} \int_0^{w^+} g(w,\theta) \, dw \, d\theta = \frac{2\pi}{p} \alpha , \tag{12}$$

where α is a "composite pellet/target characteristic" given by

$$\alpha = \frac{M}{m} p \rho_T^2 \tag{13}$$

and incorporates (in dimensionless form) those parameters which are fixed by the selection of a specific target vehicle and pellet-pattern design. The quantity p appearing in (12) and (13) represents the probability than any one pellet produces a kill, while ρ_T in (13) is the normalized radius of the effective target circle and is defined as

$$\rho_T = \frac{r_T}{(\sigma_x \sigma_y)^{\frac{1}{2}}} . \tag{14}$$

*The notation $g(w,\theta)$ expresses the fact that the expected number of pellet hits on the target depends upon the precise location of the target within the pellet array.

A simplifying assumption relating to Equation (10) is now made—namely, that each of the i particles which hit the target has the same probability p of producing a kill.* This gives for the probability that the target will be destroyed, conditional upon its receiving exactly i hits:

$$P\{\text{Kill}\,|\,i\ \text{Hits}\} = 1 - (1-p)^i \ , \quad i = 0, 1, 2, \ldots \ . \tag{15}$$

Combining Equations (10) and (15) and performing a summation (over i) so as to account for every possible grouping of pellets which might be encountered, one obtains the intrinsic effectiveness function $h(w,\theta)$:

$$\begin{aligned} h(w,\theta) &= P\{\text{Kill}\,|\,\text{Intercept}\} \ , \\ &= \sum_{i=0}^{\infty} \frac{g^i e^{-g}}{i!}[1 - (1-p)^i] \ , \\ &= 1 - e^{-pg(w,\theta)} \ . \end{aligned} \tag{16}$$

Equation (16) and the integrand in Equation (7a) are now inserted into Equation (8) to obtain the Kill Probability as

$$P\{\text{Kill}\} = \frac{1}{4\pi}\int_0^{2\pi}\int_0^{w^\dagger} [1 - e^{-pg(w,\theta)}] \exp[-\frac{w}{2\beta}(\cos^2\theta + \beta^2\sin^2\theta] \, dw \, d\theta \ , \tag{17}$$

in which the normalized average number of pellet hits (or pellet distribution function) $g(w,\theta)$ must satisfy Equation (12). The constants β and K above, representing the ratio of the standard deviations and the ratio of pellet-pattern axis lengths, are defined in (5a) and (5b), respectively. It is noted that K has the value unity for the circular lamina pattern shown in Figure 1, while β is unity for the case of identically distributed horizontal and vertical error components—that is, when the radial distribution of miss distance has no angular dependence.

In the next section Equation (17) is extremized for the special case of K and β both equal to unity to determine the ideal form of the pellet distribution function $g(w,\theta)$. Each of the functions sketched in Figure 1 is then investigated in turn for various K and β values. A discussion is included of the manner in which these so-called optimum distributions are determined, and

*Limitations introduced by this assumption are considered in Section 10.

the resulting Kill Probabilities for paraboloidal and cylindrical distributions are compared with one another.

5. Geometric Form of the Ideal Pellet Distribution Function

In order to determine the mathematical form of that distribution function which leads to the greatest overall Kill Probability, a simplified version of Equation (17) is considered: that which prevails when the components of the composite error variance are equal ($\beta=1$) and the lamina pattern is circular ($K=1$). Under these conditions, Equation (17) reduces to

$$P\{\text{Kill}\} = \frac{1}{2}\int_0^{\rho_P^2} [1 - e^{-pg(w)}]\, e^{-w/2}\, dw \quad , \qquad (K=1,\ \beta=1) \tag{18}$$

and the constraint equation (12) for the pellet distribution function $g(w)$ becomes

$$\int_0^{\rho_P^2} g(w)\, dw = \alpha/p \quad . \qquad (K=1,\ \beta=1) \tag{19}$$

In the above, ρ_P is the normalized pellet-pattern radius given by

$$\rho_P = \frac{r_P}{(\sigma_x\sigma_y)^{\frac{1}{2}}} \quad , \tag{20}$$

and the distribution function $g(w)$ represents a surface of revolution.

To extremize Equation (18) subject to the auxiliary condition (19) is now a simple isoperimetric problem in the calculus of variations. With the aid of a Lagrange multiplier to include the constraint and the appropriate Euler variational equation, one obtains for the optimum pellet distribution function* in this case the paraboloid of revolution

$$g(w)_{op} = \frac{1}{p}\left(\frac{\alpha}{\frac{\rho_P^2}{2}} + \frac{\rho_P^2}{4} - \frac{w}{2}\right) \quad , \quad w \le \rho_P^2 \quad . \qquad (K=1,\ \beta=1) \tag{21}$$

We have now reached the goal of this section, and have found the ideal form of the distribution function to be a paraboloid. However, it may be of interest to continue with this simplified case somewhat further. We will

*The designation "optimum" pellet distribution is used herein to denote that function which gives categorically the largest Kill Probability.

establish the Kill Probability for this case and then maximize it with respect to the normalized pattern radius.

Introduction of (21) into (18) leads immediately to the desired optimum Kill Probability—namely,

$$P\{\text{Kill}\}_{op} = (1 - e^{-\rho_P^2/2}) - \frac{1}{2}\rho_P^2 e^{-(\alpha/\rho_P^2 + \rho_P^2/4)} . \qquad (K=1,\ \beta=1) \tag{22}$$

A plot of this expression versus the normalized pattern radius $\underline{\rho}_P$ for three values of the dimensionless parameter $\underline{\alpha}$ is contained in Figure 5 (see $\beta=1$ curves).

The Kill Probability in (22) can now be maximized with respect to $\underline{\rho}_P$. Since $P\{\text{Kill}\}_{op}$ in Equation (22) is a monotonic increasing function of $\underline{\rho}_P^2$, no relative maximum exists. Rather, the largest possible value for the Kill Probability is sought. The distribution function in Equation (21) must, of course, be non-negative. On the boundary of the circular lamina, $w = \rho_P^2$ and $g(\rho_P^2)_{op} = \alpha/\rho_P^2 - \rho_P^2/4$. Since $g(\rho_P^2)_{op} \geq 0$, this means that $\rho_P \leq (4\alpha)^{1/4}$. Since the Kill Probability is largest for the maximum permissable radius $\underline{\rho}_P$, we take

$$\rho_P]_{max} = (4\alpha)^{1/4} \qquad (K=1,\ \beta=1) \tag{23}$$

and obtain

$$P\{\text{Kill}\}_{op}]_{max} = 1 - (1 + \sqrt{\alpha})\, e^{-\sqrt{\alpha}} . \qquad (K=1,\ \beta=1) \tag{24}$$

Graphs of Equations (23) and (24) versus $\underline{\alpha}$ are to be found in Figures 6 and 7, respectively. The pellet distribution function accompanying the maximum Kill Probability above is found by substituting (23) into (21):

$$g(w)_{op}]_{max} = \frac{1}{p}\left(\sqrt{\alpha} - \frac{w}{2}\right) , \quad 0 \leq w \leq 2\sqrt{\alpha} . \qquad (K=1,\ \beta=1) \tag{25}$$

One notes that the above surface is identically zero on the boundary of the circular lamina, that is, when $w = 2\sqrt{\alpha}$.

The significant feature of the foregoing analysis is the shape of the pellet distribution function: a paraboloid. Furthermore, the Kill Probability is seen to be largest for a specific value of the pattern dimension.

It is now assumed, with Morse and Kimball [2], that the ideal pellet distribution is also paraboloidal for non-symmetrical components of the composite error variance, i.e., for $\beta \neq 1$. However, the particular shape of the paraboloidal surface, as well as its boundary configuration, is not necessarily similar to that considered above for $\beta=1$. These properties must be determined anew, and indeed separately for the two lamina types $K=1$ and $K\neq 1$. For $K=1$ the optimum distribution function is found to be an elliptic paraboloid which is not identically zero on the boundary of the circular lamina while an elliptic paraboloid which is identically zero on the boundary of the elliptical lamina is found for $K\neq 1$. These results are depicted in Figure 1a and analyzed in the following section.

6. Optimum Paraboloidal Pellet Distribution Functions

In the event $\beta\neq 1$ (so that the radial distribution of miss distance has an angular dependence), that paraboloidal distribution function (the optimum paraboloid) is to be determined which yields the largest Kill Probability subject to the subsidiary condition of Equation (12). Both the circular lamina ($K=1$) and the elliptical lamina ($K\neq 1$) are considered. To begin with, the distribution function is taken in the general paraboloidal form

$$g(w,\theta) = A - w\,(B \sin^2\theta + C \cos^2\theta) \quad , \tag{26}$$

where A, B, and C are constants to be determined. Substitution of (26) into (12) leads to the first equation relating these constants:

$$A = \frac{K\alpha}{p\rho_a^2} + \frac{\rho_a^2}{4K^2}\,(B + CK^2) \quad . \tag{27}$$

It is next reasoned that the elliptical cross-sections of the surface (26) should optimally have the same shape (eccentricity) as the elliptic error pattern; in other words, the mean density of pellets should be constant along a curve whose probability density is constant. This gives

$$(1 - B/C)^{\frac{1}{2}} = (1 - \beta^2)^{\frac{1}{2}} \quad , \tag{28a}$$

or

$$B = \beta^2 C \quad . \tag{28b}$$

Substitution of (28b) into (27) results in the following relationship between A and C:

$$(29) \qquad A = \frac{K\alpha}{p\rho_a^2} + \frac{\rho_a^2}{4K^2} C (\beta^2 + K^2) \quad .$$

A third equation associating A, B, and C will be determined separately for the cases $K \neq 1$ and $K = 1$.

Since the probability density function is a smooth function decreasing with increasing distance from the center of the distribution, it is reasoned that the pellet distribution function must likewise be a smooth function. For the elliptical lamina ($K \neq 1$), one then requires that the pellet distribution function (26) be identically equal to zero (in θ) on the boundary of the lamina—that is,

$$(30) \qquad g\left[\frac{\rho_a^2}{\cos^2\theta + K^2 \sin^2\theta}, \theta\right] \equiv 0$$

for all θ. This is in agreement with a similar condition determined in the previous section, which led to the optimum Kill Probability for a circular lamina ($K=1$) and a circular error pattern ($\beta=1$). With the use of (26) and (29), one obtains from condition (30) the fact that K must equal β and also that

$$(31) \qquad C = \frac{2\beta\alpha}{p\rho_a^4} \quad .$$

Upon finding A from (29), use of (28b) and (31) gives for the optimum paraboloidal distribution function,

$$(32) \qquad g(w,\theta)_{op} = \frac{2\beta\alpha}{p\rho_a^2}\left[1 - \frac{w}{\rho_a^2}(\cos^2\theta + \beta^2\sin^2\theta)\right] \quad . \qquad (K=\beta)$$

Equation (17) for the Kill Probability now reduces, with the substitution of Equation (32), to the form

$$(33) \qquad P\{Kill\}_{op} = (1 - e^{-\rho_a^2/2\beta}) - \frac{e^{-2\beta\alpha/\rho_a^2} - e^{-\rho_a^2/2\beta}}{1 - \frac{4\alpha\beta^2}{\rho_a^4}} \quad . \qquad (K=\beta)$$

A graph of $\underline{P}\{\text{Kill}\}_{op}$ versus $\rho_a/\beta^{\frac{1}{2}}$ for various $\underline{\alpha}$ values is shown in Figure 3. (This figure also contains the corresponding curve for the optimum cylindrical distribution discussed in the following section.) Maximum Kill Probabilities are obtained by differentiating (33) with respect to $\underline{\rho_a^2}$ and equating the result to zero. Thus, one obtains as the normalized semiaxis lengths of that elliptical lamina which yields maximum Kill Probability

$$\rho_a]_{max} = \beta^{\frac{1}{2}} (4\alpha)^{1/4} \quad , \qquad (K\approx\beta) \tag{34a}$$

$$\rho_b]_{max} = \frac{1}{\beta^{\frac{1}{2}}} (4\alpha)^{1/4} \quad . \tag{34b}$$

The maximum value of Equation (33) is

$$P\{\text{Kill}\}_{op}]_{max} = 1 - (1 + \sqrt{\alpha})\, e^{-\sqrt{\alpha}} \quad , \qquad (K\approx\beta) \tag{35}$$

a result identical with that for K=1 and β=1 as found in Equation (24). This function, which is independent of $\underline{\beta}$, is plotted in Figure 7, while $\rho_a]_{max}/\beta^{\frac{1}{2}}$ is depicted in Figure 4. (A corresponding graph for the optimum cylindrical distribution is also shown.) The pellet distribution function accompanying the above maximum is found by introducing (34a) into (32):

$$g(w,\theta)_{op}]_{max} = \frac{1}{p}\left[\sqrt{\alpha} - \frac{w}{2\beta}\left(\cos^2\theta + \beta^2\sin^2\theta\right)\right] \quad . \qquad (K\approx\beta) \tag{36}$$

For the circular lamina (K=1), Equations (28b) and (29) remain applicable. However, the boundary condition differs from that considered above. The pellet distribution function is now required to be zero at but two opposite points on the boundary of the circular lamina—namely, those points on a line coinciding with the minor axis of the error ellipse. This corresponds to vectorial angles $\underline{\theta}$ of 0° and 180°; selecting one of these, we write

$$g(\rho_p^2,\ 0^\circ) = 0 \quad , \tag{37}$$

in which $\underline{\rho_p}$ is the normalized radius of the circular lamina. (The 180° angle would give the same result.) Condition (37) in conjunction with Equation (29) and $\underline{K}$ equal to unity determines the constant $\underline{C}$ in this case:

$$C = \frac{4\alpha}{p\rho_p^4(3 - \beta^2)} \quad . \tag{38}$$

With $\underline{A}$ in Equation (29) now completely determined, one can specify the optimum paraboloidal distribution function with the aid of (28b) and (38). There results

$$(39) \qquad g(w,\theta)_{op} = \frac{4\alpha}{p\rho_P^2(3-\beta^2)}\left[1 - \frac{w}{\rho_P^2}(\cos^2\theta + \beta^2\sin^2\theta)\right] . \qquad (K=1)$$

Equation (17) for the Kill Probability then becomes with K=1,

$$(40) \quad P\{Kill\}_{op} = \frac{1}{4\pi}\int_0^{2\pi}\int_0^{\rho_P^2}[1-e^{-pg(w,\theta)_{op}}]\exp[-\frac{w}{2\beta}(\cos^2\theta + \beta^2\sin^2\theta)]\,dw\,d\theta .$$

In Appendix B, each of the double integrals appearing in (40) is reduced to the form tabulated by Cox and Johnson [3].* Thus, indicating the tabulated integrals by $\underline{P}_{TAB}$,

$$(41) \qquad P\{Kill\}_{op} = P_{TAB}(k,A_P) - (\frac{A_P}{B_P})^2 e^{-\frac{1}{2}(A_P^2 - B_P^2)} P_{TAB}(k,B_P) , \qquad (K=1)$$

where

$$(42) \qquad k = 1/\beta ,$$

$$(43) \qquad A_P = \rho_P/\beta^{\frac{1}{2}} ,$$

$$(44) \qquad B_P = A_P\left[1 - \frac{8\alpha}{\beta(3-\beta^2)A_P^4}\right]^{\frac{1}{2}} .$$

Equation (41) is valid for all $\underline{\beta}$, including $\beta=1$, and is plotted in Figure 5 versus $\underline{\rho}_P$ for various values of $\underline{\beta}$ and three values of the parameter $\underline{\alpha}$ defined in Equation (13). Maximum Kill Probabilities occurring in Figure 5 are plotted versus $\underline{\alpha}$ in Figure 7. The corresponding normalized pattern radius values, $\underline{\rho}_P]_{max}$, are shown in Figure 6 as a function of $\underline{\alpha}$. The maximum Kill Probability plot for $\beta=1$ in Figure 7 coincides with the curve representing, for all $\underline{\beta}$ values, the optimum paraboloidal distribution for elliptical laminas.

Attention is drawn to the values in Figure 5 indicated by arrows. These represent Kill Probabilities which would be realized if one were to base the pellet-pattern design on the assumption of equal components for the composite

*A more extensive but as yet unpublished set of tables was provided the authors by Herbert Solomon, Stanford University, in a private communication.

error variance. For large $\underline{\alpha}$ values, a marked degradation in Kill Probability is noted over that to be had by adequately accounting for the error-pattern eccentricity. Of course, the more eccentric the error pattern, the more important it becomes to consider its ellipticity in the design of the pellet array.

In the following section, the optimum cylindrical distribution functions depicted in Figure 1b are analyzed for comparison with the optimum paraboloidal distributions considered thus far. Figure 7 contains plots of the maximum Kill Probability attainable with an optimum cylinder, as well as curves relating to the optimum paraboloid of revolution of Figure 1c; the latter is discussed in Section 8 prior to an evaluation of the overall conclusions to be had from studies of the several distributions.

7. Optimum Cylindrical Pellet Distribution Functions

The cylindrical pellet distributions shown in Figure 1b are treated next for both the elliptical lamina ($K\neq 1$) and the circular lamina ($K=1$). With the distribution of pellets regarded as a constant $\underline{G}$ throughout the lamina, that is, with

$$g(w,\theta) \equiv G \quad , \tag{45}$$

the constraint equation (12) leads immediately to the expression

$$G = K\frac{\alpha}{p\rho_a^2} \quad , \tag{46}$$

where $\underline{\rho_a}$ and $\underline{\rho_p}$ are synonymous in the case of a circular lamina ($K=1$). Equation (17) for the Kill Probability now becomes

$$P\{\text{Kill}\} = \frac{1}{4\pi}(1 - e^{-K\alpha/\rho_a^2}) \int_0^{2\pi}\int_0^{w^\dagger} \exp[-\frac{w}{2\beta}(\cos^2\theta + \beta^2\sin^2\theta)]\ dw\ d\theta \quad . \tag{47}$$

This result will be examined separately for the elliptical and circular laminas.

In the elliptical lamina case ($K\neq 1$), one wishes to find the ratio $\underline{K}$ of pattern axis lengths such that the Kill Probability in (47) is optimum. Therefore, the following heuristic argument is introduced. Since the distribution function is a constant for a fixed pattern area, the Kill Probability is

largest when the Hit Probability is largest. Since the latter occurs when the pellet pattern coincides with a locus of constant probability density, the shape (eccentricity) of the pellet pattern must be identical to that of the error pattern— that is, $\underline{K}$ must equal $\underline{\beta}$ for optimum Kill Probability. Equation (47) then reduces to

$$(48) \qquad P\{\text{Kill}\}_{op} = (1 - e^{-\beta\alpha/\rho_a^2})\,(1 - e^{-\rho_a^2/2\beta}) \quad , \qquad (K=\beta)$$

which is shown plotted versus $\rho_a/\beta^{\frac{1}{2}}$ for several values of $\underline{\alpha}$ in Figure 3. The maximum value in Equation (48) is found by differentiating with respect to $\underline{\rho_a}$, and is given by

$$(49) \qquad P\{\text{Kill}\}_{op}]_{max} = (1 - e^{-\sqrt{\alpha/2}})^2 \quad , \qquad (K=\beta)$$

a result independent of $\underline{\beta}$. A graph of this maximum Kill Probability versus $\underline{\alpha}$ is contained in Figure 7. The corresponding normalized semiaxis lengths of the elliptical lamina are

$$(50a) \qquad \rho_a]_{max} = \beta^{\frac{1}{2}}(2\alpha)^{1/4} \quad , \qquad (K=\beta)$$

$$(50b) \qquad \rho_b]_{max} = \frac{1}{\beta^{\frac{1}{2}}}(2\alpha)^{1/4} \quad ;$$

a plot of $\rho_a]_{max}/\beta^{\frac{1}{2}}$ versus $\underline{\alpha}$ is found in Figure 4.

In the circular lamina case (K=1), Equation (47) can be reduced to a tabulated form as shown in Appendix B; the result is

$$(51) \qquad P\{\text{Kill}\}_{op} = (1 - e^{-\alpha/\rho_P^2})\, P_{TAB}(k, A_P) \quad , \qquad (K=1)$$

where $\underline{k}$ and $\underline{A_P}$ are defined in Equations (42) and (43), respectively. Plots of Equation (51) are found in Figure 8, and the maximum is again plotted versus $\underline{\alpha}$ in Figure 7. The maximum Kill Probability for $\beta=1$ in this case coincides with that obtained for all $\underline{\beta}$ in the above case of the optimum cylindrical distribution throughout an elliptical lamina. Maxima in the present case occur for pellet-pattern radii given by the curves of Figure 9. As in Figure 5, the values indicated by arrows in Figure 8 represent Kill Probabilities which would be realized if one were to design the pellet pattern on the assumption of equal components for the composite error variance. Once again, a

decided degradation in Kill Probability is evidenced for relatively large α values, especially in the cases of highly eccentric error ellipses.

8. The Optimum Paraboloid of Revolution as a Pellet Distribution Function

It is of interest to investigate the Kill Probability resulting from the use of an optimum paraboloid of revolution as the pellet distribution within a circular lamina ($K=1$). For identical components of error variance ($\beta=1$), the present case is identical to that for a circular lamina considered in Section 6. With $\beta\neq 1$, the two cases differ as revealed by comparing Figure 1a (circular lamina) with Figure 1c.

One begins here by considering as the distribution function a paraboloid of revolution in the general form

$$g(w,\theta) = D - Ew \quad , \tag{52}$$

where D and E are constants to be determined such that the Kill Probability for this distribution is optimum. The first equation relating the above constants is obtained immediately by imposing condition (12) on the distribution (52), which gives

$$D = \frac{\alpha}{p\rho_P^2} + E\frac{\rho_P^2}{2} \quad . \tag{53}$$

Here ρ_a in Equation (12) is replaced by the pellet-pattern radius ρ_P as defined by Equation (20). A second relation between D and E may be derived by virtue of an argument similar to that advanced in Section 6. Thus, the optimum boundary condition on (52) is

$$g(\rho_P^2,\theta) \equiv 0 \tag{54}$$

for all θ— that is, the distribution of pellets vanishes on the circumference of the circular lamina. Then $D = E\rho_P^2$ which, combined with (53), gives

$$D = 2\alpha/p\rho_P^2 \quad , \tag{55a}$$

$$E = 2\alpha/p\rho_P^4 \quad . \tag{55b}$$

Therefore, the optimum paraboloid of revolution becomes

$$(56) \qquad g(w,\theta)_{op} = \frac{2\alpha}{p\rho_P^4}\,(\rho_P^2 - w) \ .$$

Equation (17) giving the Kill Probability has the following form when Equation (56) is substituted therein:

$$(57) \quad P\{\text{Kill}\}_{op} = P_{TAB}(k,A_P) - \frac{e^{-2\alpha/\beta A_P^2}}{4\pi}\int_0^{2\pi}\int_0^{\beta A_P^2} \exp\left[\frac{w}{2}\left(\frac{4\alpha}{\beta^2 A_P^4} - \beta\sin^2\theta - \frac{1}{\beta}\cos^2\theta\right)\right] dw\, d\theta \ ,$$

where $k = 1/\beta$ and $A_P = \rho_P/\beta^{1/2}$ as defined by Equations (42) and (43), respectively. The non-tabulated integral in (57) can be evaluated approximately by utilizing Simpson's Rule; the resulting Kill Probability is plotted versus the normalized pattern radius ρ_P for several α and β values in Figure 10. Maximum Kill Probabilities occur at the particular pattern radii shown in Figure 11, and have the magnitudes indicated by the appropriate plots in Figure 7. Values indicated by arrows in Figure 10 are the Kill Probabilities realized with a distribution function designed to be optimum in the case of identical error-variance components ($\beta=1$). Relatively large gains are achieved in predicted Kill Probability, especially for large α and small β values, if the design includes the optimum paraboloid of revolution as the pellet distribution function in this case.

9. Summary of the Mathematical Analysis

The foregoing mathematical study has been concerned with determining kill probabilities for various spatial distributions of pellets throughout both circular and elliptical laminas. Three classes of pellet distributions were considered, which reference to Figure 1 will recall to the reader. They consist of those paraboloidal, cylindrical, and paraboloid-of-revolution configurations which were found to lead to the optimum kill probability. Probable errors of predicting target position and of placing the pellet pattern at that position have been included, but errors due to improper orientation of the pellet lamina with respect to the target at interception have been ignored.

A composite pellet/target characteristic $\underline{\alpha}$ has been introduced to account for target size (assumed small as compared with that of the pellet lamina), individual pellet mass, overall mass, and the kill probability of a single pellet which hits the target. Each pellet is regarded as having the same chance of destroying the target as had its predecessor. (An assessment of this hypothesis is contained in the following section.

It was found, in each of the several pellet distribution cases, that the optimum Kill Probability could be maximized with respect to the size of the pellet lamina. The maximum Probability was seen always to be a monotonic increasing function of the parameter $\underline{\alpha}$. This means that if we consider the weapon-target combination to fix the total pellet mass and the normalized effective target radius, a weapon design objective would be to select the individual pellet mass such that $\underline{\alpha}$ is as large as possible. It is noted that this selection entails a determination of an empirical relationship between the kill probability and the mass of a single pellet.

An anticipated result of the analysis is that the paraboloidal pellet distribution throughout an elliptical lamina of optimum dimensions (and eccentricity equal to that of the error ellipse) indeed affords the largest expected Kill Probability. However, the optimum cylindrical distribution over an elliptical lamina was found to give almost as large Kill Probabilities, especially in the extremes of relatively small or large $\underline{\alpha}$ values. With a circular lamina, the optimum paraboloidal distribution reveals a significantly larger maximum Kill Probability than does the optimum cylindrical distribution when the error pattern has a large eccentricity ($\underline{\beta}$ less than one half). In fact, the optimum paraboloid of revolution as a distribution, while not entirely as promising as the elliptical paraboloid, was also found to be superior to the cylindrical distribution in yielding larger Kill Probabilities.

Paraboloidal distributions allow for considerably broader crests in the curves of Kill Probability versus pellet-pattern size than do cylindrical distributions. This difference becomes more pronounced as the composite pellet/target characteristic $\underline{\alpha}$ increases. The paraboloid-of-revolution configuration leads to wider crests in the Kill Probability graphs than does the elliptical paraboloid over a circular lamina, thus revealing the more critical nature of

the pellet-pattern size in the latter case. In general with any of the distributions, the more eccentric the error pattern, the broader the Probability peaks become.

The dimensions of the lamina pattern which give, for each distribution, the maximum Kill Probability are monotonic functions of α. No precise dependence of optimum dimensions on error-pattern axis ratio β can be deduced on the whole. However, for circular laminas, as β decreases, the optimum pattern size decreases for small α and increases for large α. This phenomenon is the natural result of "placing the pellets where they do the most good." If α is small, the optimum pattern size diminishes as the error pattern becomes more eccentric, so that the relatively few pellets available can be concentrated in a region of higher probability density; the important factor in this case is to obtain sufficient hits on the target. On the other hand, if α is quite large, the larger the error-pattern eccentricity the larger the optimum pellet lamina to insure target interception; since the density of pellets in this latter case is high, interception is the significant factor.

10. Assessment of the "Vital-Spot Hypothesis"

A basic assumption in this paper is that the kill probability p of a pellet which hits the target is a constant ($0 < p \leq 1$), independent of the number of pellets hitting the target. This assumption, referred to by Morse and Kimball [2] as the "vital-spot hypothesis," has been found to give satisfactory results in many cases and seems fairly realistic, for example, when applied to targets involving electro-mechanical assemblies. It is of interest, however, to investigate the applicability of this hypothesis in the case of certain other targets (among which live targets are a prime example) for which the kill probabilities of the individual pellets have the following property:

$$p_1 \leq p_2 \leq \cdots \leq p_{j-1} \leq p_j \leq p_{j+1} \leq \cdots , \tag{58}$$

that is, each pellet has a greater chance of disabling the target than has its predecessor. The individual pellet kill probabilities can be expressed in the following form:

$$
\begin{aligned}
&p_0 = 0 \ , \\
(59) \qquad &p_1 = p \ , \\
&p_j = p_{j-1} + c_j(1-p_{j-1}) \ , \ j \geq 2 \ ,
\end{aligned}
$$

where the c_j's are empirical constants in the range $0 \leq c_j \leq 1$.

A model of intermediate complexity which may be a good approximation to the above case is on for which $c_2 = c_3 = \ldots = c$. This model involves only the two constants p and c. Under this assumption of equal c_j's, the results in (59) reduce to

$$
\begin{aligned}
&p_0 = 0 \ , \\
(60) \qquad &p_1 = p \ , \\
&p_j = p_{j-1} + c(1 - p_{j-1}) = c + p_{j-1}(1 - c) \ , \ j \geq 2 \ .
\end{aligned}
$$

For convenience, Equations (60) may be expressed in terms of $q_j = 1 - p_j$ as follows:

$$
\begin{aligned}
&q_0 = 1 \ , \\
(61) \qquad &q_1 = 1 - p \ , \\
&q_j = (1 - c)^{j-1} (1 - p) \ , \ j \geq 2 \ .
\end{aligned}
$$

It is proposed to compare the results of this paper, which are predicated upon the vital-spot assumption, with results obtainable from the aforementioned model, and thereby to establish some "limits of applicability" on the analysis previously presented. Since the maximum Kill Probabilities for the paraboloidal distribution discussed earlier do not differ significantly from those obtained with the cylindrical distribution, the latter alone are considered here.

In view of Equations (61), the effectiveness function $h(w,\theta)$ for the cylindrical pellet distribution no longer has the form given in Equation (16). Instead,

$$
(62) \qquad h(w,\theta) = \sum_{i=0}^{\infty} \left(\frac{g^i e^{-g}}{i!}\right) \left(1 - \prod_{j=0}^{i} q_j\right) \ ,
$$

which becomes, upon introduction of (61),

$$(63) \quad h(w,\theta) = 1 - e^{-g}\,[1 + g(1-p)] - \sum_{i=2}^{\infty} \left(\frac{g^i e^{-g}}{i!}\right)(1-p)^i \prod_{j=2}^{i} (1-c)^{j-1} \quad .$$

In the above, g represents the expected number of pellets striking the target. Equation (63) can also be written as

$$(64) \quad h(w,\theta) = 1 - e^{-g}\left[1 + g(1-p) + \sum_{i=2}^{\infty} \frac{g^i (1-p)^i}{i!}(1-c)^{i(i-1)/2}\right] \quad ,$$

whereupon two special cases, $c = 0$ and $c = 1$, are immediately expressible in the simplified form

$$(65a) \quad h(w,\theta) = 1 - e^{-pg} \quad , \qquad (c = 0)$$

$$(65b) \quad h(w,\theta) = 1 - e^{-g}\,[1 + g(1-p)] \quad . \qquad (c = 1)$$

Equation (65a) corresponds to the result of the vital-spot hypothesis (the kill probability of each pellet is the same) and is Equation (16) of the text. Equation (65b) represents the opposite extreme-that is, the second pellet (and all subsequent ones) is certain to kill the target upon striking it. Figures 12 and 13 present the effectiveness function of Equation (64) plotted versus the mean number of target hits g for pellet kill probabilities p of 0.1 and 0.5, respectively. Shown are graphs for c values of 0, 0.1, 0.5, and 1.0 which thus include the extreme cases of Equations (65).

A measure of the general applicability of the vital-spot theory is obtained by comparison of the maximum Kill Probability attainable for $c=0$ with that for $c\neq 0$. This can be accomplished by choosing the circular lamina pattern of Figure 1b ($K=1$) and a symmetrical error distribution ($\beta=1$). Under these circumstances the Kill Probability for the uniform pellet distribution is, from Equation (8),

$$(66) \quad P\{\text{Kill}\} = h(w,\theta)\,(1 - e^{-\rho_P^2/2}) \quad ,$$

where $h(w,\theta)$ is given by (64) and ρ_P^2 is the normalized pellet-lamina radius defined in Equation (20). Since the distribution function g must satisfy the restriction expressed by Equation (12), its value is found from Equation (46) to be

$$(67) \quad g = \frac{a}{p\rho_P^2} \quad .$$

With $c = 0$, the effectiveness function is given by Equation (65a); the accompanying Kill Probability in (66) can be maximized by differentiation with respect to $\underline{\rho}_P$. There results

$$P\{\text{Kill}\}_{max} = (1 - e^{-\sqrt{a/2}})^2 \quad ; \qquad (c = 0) \tag{68}$$

the value of $\underline{\rho}_P$ which yields this maximum is

$$\rho_P]_{max} = (2\alpha)^{1/4} \quad . \qquad (c = 0) \tag{69}$$

With $c \neq 0$, the effectiveness function in (66) is represented by the graphs of Figures 12 and 13. Maximum Kill Probabilities are obtained by trial and error procedures. Table 1 summarizes maximum Kill Probabilities and optimum pattern radii obtained for several values of $\underline{c}$, $\underline{\alpha}$, and $\underline{p}$, including $c = 0$.

Table 1. Maximum Kill Probabilities and Optimum Normalized Pattern Radii for Several Values of Pellet Tandem Factor $\underline{c}$.

c	α / p	1		5		10	
		$P\{\text{Kill}\}_{max}$	$\rho_P]_{max}$	$P\{\text{Kill}\}_{max}$	$\rho_P]_{max}$	$P\{\text{Kill}\}_{max}$	$\rho_P]_{max}$
0	0.1	0.26	1.2	0.63	1.8	0.80	2.1
0.1		0.45	1.3	0.89	2.4	0.97	2.8
0.5		0.60	1.6	0.95	2.6	0.99	3.2
1.0		0.67	1.7	0.97	2.8	0.995	3.5
0	0.5	0.26	1.2	0.63	1.8	0.80	2.1
0.1		0.26	1.2	0.65	1.8	0.82	2.2
0.5		0.28	1.2	0.68	1.9	0.85	2.3
1.0		0.30	1.1	0.71	1.9	0.87	2.3

The following conclusions are evident from an inspection of Table 1. For large values of $\underline{p}$, say one half or larger, the vital-spot hypothesis appears in general to be an adequate assumption. In this case, values of $\underline{c}$ even as large as unity yield maximum Kill Probabilities and optimum pattern radii differing by no more than about 10 percent from those based on zero $\underline{c}$. However,

for values of p less than a half, the vital-spot assumption may lead to results differing somewhat from those obtained with the model considered in this section, especially for small p and large values of pellet tandem factor c. When p=0.1, for example, even small values of c such as 0.1 yield Kill Probabilities which are significantly different from that realized with c=0.

11. Application to a Shotgun-Bird System

Results of the foregoing mathematical development are now applied to a specific weapon-target system consisting of shotgun and bird, and a study is made of the theoretical Kill Probability for a proposed shell and gun design.

As noted earlier, an objective in the design of a pellet-dispersing shell should be the maximization of the ratio p/m of individual pellet kill probability to pellet mass. This presupposes a knowledge of the target type and the nominal range-to-target, and entails a determination of an empirical relationship between the individual kill probability and the mass of a single pellet. We propose such an optimum shell design, and tabulations of the individual pellet mass m to be chosen and the accompanying optimum ratio of p/m for various birds and nominal ranges. Thus, one can select the proper shell for a given "job." If, for a given gun, one's error variances σ_x^2 and σ_y^2 are known, the composite pellet/target characteristic α is then ascertainable, as well as the ratio β of standard deviations.

Present shotguns are built to project a circular pellet array. We propose a "gun choke" which can shape the shot pattern into an elliptical lamina of eccentricity equal to that predicted for the error ellipse.* Furthermore, the choke is to be "rotatable" in order that the major axis of the shot pattern can be aligned with the major axis of the error ellipse, where the latter is considered as the projection of the flight path (assumed

*It is tacitly assumed that, over the time interval between firing of the shotgun and target interception, the shot pattern retains its initial shape although increasing uniformly and symmetrically in size.

to be rectilinear) of the bird into the pellet plane.* A gun choke setting is also incorporated which allows for optimum pellet-pattern size at interception and which is based upon estimates of α and β.

If, for a given type of bird, the range-to-target, target size, and the composite error variances could be accurately predicted, and if the shell design were perfect, an exact α and β could be determined, and hence one could expect the maximum Kill Probabilities displayed in Figure 7. Since precise prediction of the above parameters is impossible, the gun choke setting will generally be inaccurate, and hence the pattern size at intercept will not be optimum. We therefore consider pattern sizes at impact to vary by as much as 50% about the optimum.

In our present application, a representative pellet mass m of 0.01 ounce is taken, and the fairly realistic value of 0.50 is chosen for p, the individual pellet kill probability. (This latter value is sufficiently large that, according to the analysis in Section 10, the vital-spot theory may be regarded as applicable and hence also the results herein presented.) An effective target radius of 1/5 foot is assumed, while the overall pellet mass is 1 ounce. Computed Kill Probabilities with and without the proposed choke (that is, for elliptical and circular laminas) are to be compared for two optimally designed pellet distributions: the cylindrical and the paraboloidal. For the circular pellet array, both distributions are taken as surfaces of revolution.

Table 2 contains optimum Kill Probabilities pertaining to paraboloidal and cylindrical distributions contained within a circular lamina, for a few typical error variances, α numbers, and values of the error-pattern axis ratio β. Pellet-pattern radii at intercept are taken as 1/2, 3/4, 1, 5/4, and 3/2 of that ideal value, $r_P]_{max}$, which yields maximum Kill Probability under the given conditions. All rows of Kill Probability for which $\beta=1$ are

*All of the errors here can be attributed approximately to inaccuracy in placement of the pellet pattern on target at intercept, and these placement errors tend to be larger along the direction of target motion; hence the particular choice of major axis for the error ellipse. Consistent with the arbitrarily adopted convention $\sigma_x \leq \sigma_y$, this major axis becomes the y-axis of the rotated coordinate system introduced in Section 2.

Table 2. Kill Probabilities for a Shotgun-Bird System.

Pellet Distribution	σ_x^2 (ft^2)	σ_y^2 (ft^2)	β	α	$r_{P]max}$ (ft)	$a_{P]max}$ (ft)	$P\{Kill\}_{op}$				
							$\frac{1}{2}\, r_{P]max}$	$\frac{3}{4}\, r_{P]max}$	$r_{P]max}$	$\frac{5}{4}\, r_{P]max}$	$\frac{3}{2}\, r_{P]max}$
Optimum Paraboloidal	1/5	1/5	1	10	1.12	1.12	0.52	0.75	0.82	0.78	0.70
	1/10	2/5	1/2	10	1.15	0.79	0.50	0.71	0.77	0.73	0.66
	1/20	4/5	1/4	10	1.26	0.56	0.47	0.61	0.66	0.63	0.57
	2	2	1	1	2.01	2.01	0.16	0.25	0.27	0.25	0.23
	1	4	1/2	1	1.88	1.41	0.15	0.23	0.25	0.24	0.21
	1/2	8	1/4	1	1.78	1.00	0.12	0.19	0.22	0.20	0.18
Optimum Cylindrical	1/5	1/5	1	10	0.93	0.93	0.42	0.69	0.80	0.74	0.63
	1/10	2/5	1/2	10	0.96	0.67	0.40	0.65	0.74	0.70	0.62
	1/20	4/5	1/4	10	1.00	0.47	0.38	0.56	0.63	0.59	0.52
	2	2	1	1	1.71	1.71	0.15	0.24	0.26	0.24	0.21
	1	4	1/2	1	1.68	1.19	0.15	0.22	0.24	0.23	0.20
	1/2	8	1/4	1	1.57	0.83	0.13	0.18	0.21	0.19	0.17

also applicable to elliptical pellet laminas, irrespective of $\underline{\beta}$. In this case the symbol $\underline{r}_P]_{max}$ in the Kill Probability portion of Table 2 is to be replaced by $\underline{a}_P]_{max}$, the ideal semiminor axis length of the pellet lamina. Ideal semiminor axis lengths, which are dependent upon $\underline{\beta}$, are listed in a separate column; corresponding ideal semimajor axis lengths are equal to $a_P]_{max}/\beta$.

An examination of Table 2 indicates the special utility of the gun choke in the case of rather eccentric error ellipses ($\beta < 1/2$) and values of $\underline{\alpha}$ as large as 10. Whether the pellet distribution is paraboloidal or cylindrical, the advantageous effects of the choke are evidently about the same. When $\beta=1/4$, for example, the Kill Probability is generally larger by approximately 25% with an appropriate elliptical lamina over that accompanying the conventional circular array. Erroneous estimates of range-to-target, target size, and the composite error variances are manifested in the pellet-pattern size at intercept. Although "pattern-size errors" of less than $\pm$ 25% play a rather insignificant role, errors as large as $\pm$ 50% have a considerable effect on the Kill Probability. It is noted that a paraboloidal distribution is not as sensitive to variations in the pattern size about the optimum as is the cylindrical distribution.

The following conclusions, in order of relative importance, can now be made with respect to ways whereby a hunter may increase his kill probability:

(1) Attainment of the optimum pellet-pattern size at intercept would bring about the largest improvement in kill probability. This requires a knowledge of one's error variances, and judicious prediction of target size, range-to-target, and individual pellet kill probability.

(2) For hunters already achieving kill probabilities on the order of 0.50, further improvements can be had through the use of elliptical pellet laminas of suitable shape.

(3) Shaping of the pellet distribution to conform to an optimum paraboloid will have a twofold probable result: not only will the expected kill probability be increased, but also the detrimental effects of unavoidable non-optimum pattern sizes are minimized.

FIGURES 3 - 13

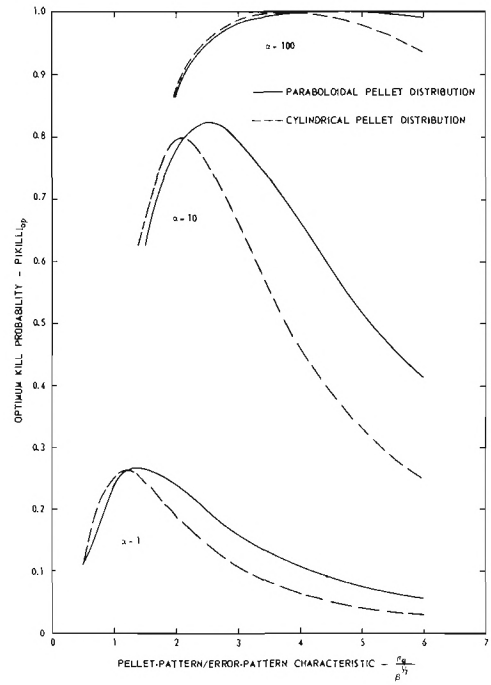

Figure 3. Kill Probability Accompanying Optimum Paraboloidal and Cylindrical Pellet Distributions Over Elliptical Laminas, for Various Values of Composite Pellet/Target Characteristic α.

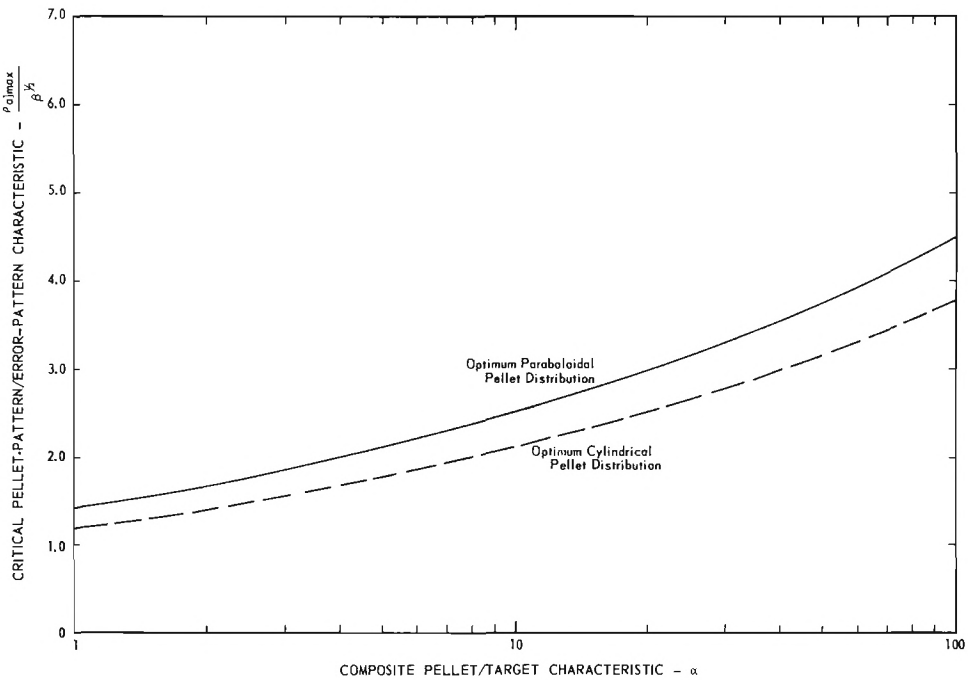

Figure 4. Normalized Semiminor Axis Length of the Elliptical Pellet Lamina Which Maximizes the Kill Probability Accompanying Optimum Paraboloidal and Cylindrical Pellet Distributions.

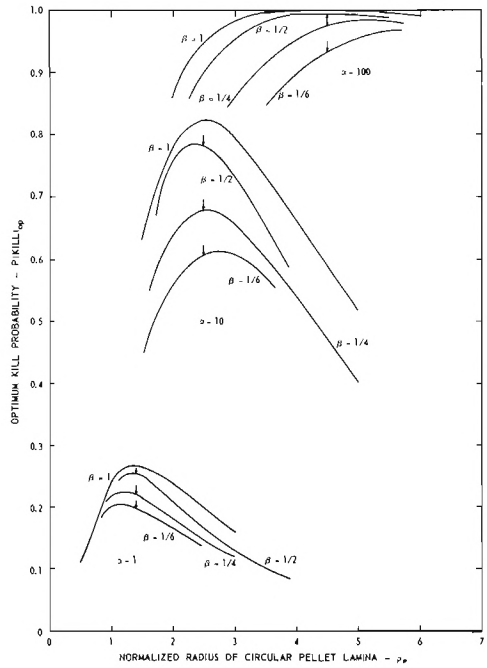

Figure 5. Kill Probability Accompanying Optimum Paraboloidal Pellet Distributions Over Circular Laminas, for Various Values of Error-Pattern Axis Ratio β and Composite Pellet/Target Characteristic α.

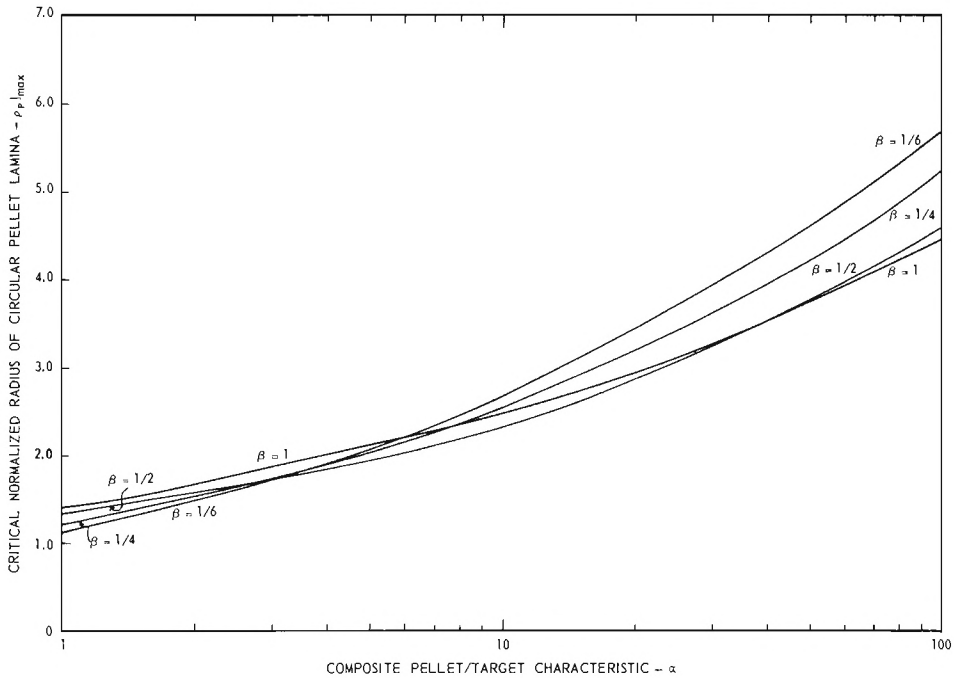

Figure 6. Normalized Radius of the Circular Pellet Lamina Which Maximizes the Kill Probability Accompanying Optimum Paraboloidal Pellet Distributions, for Various Values of Error-Pattern Axis Ratio β.

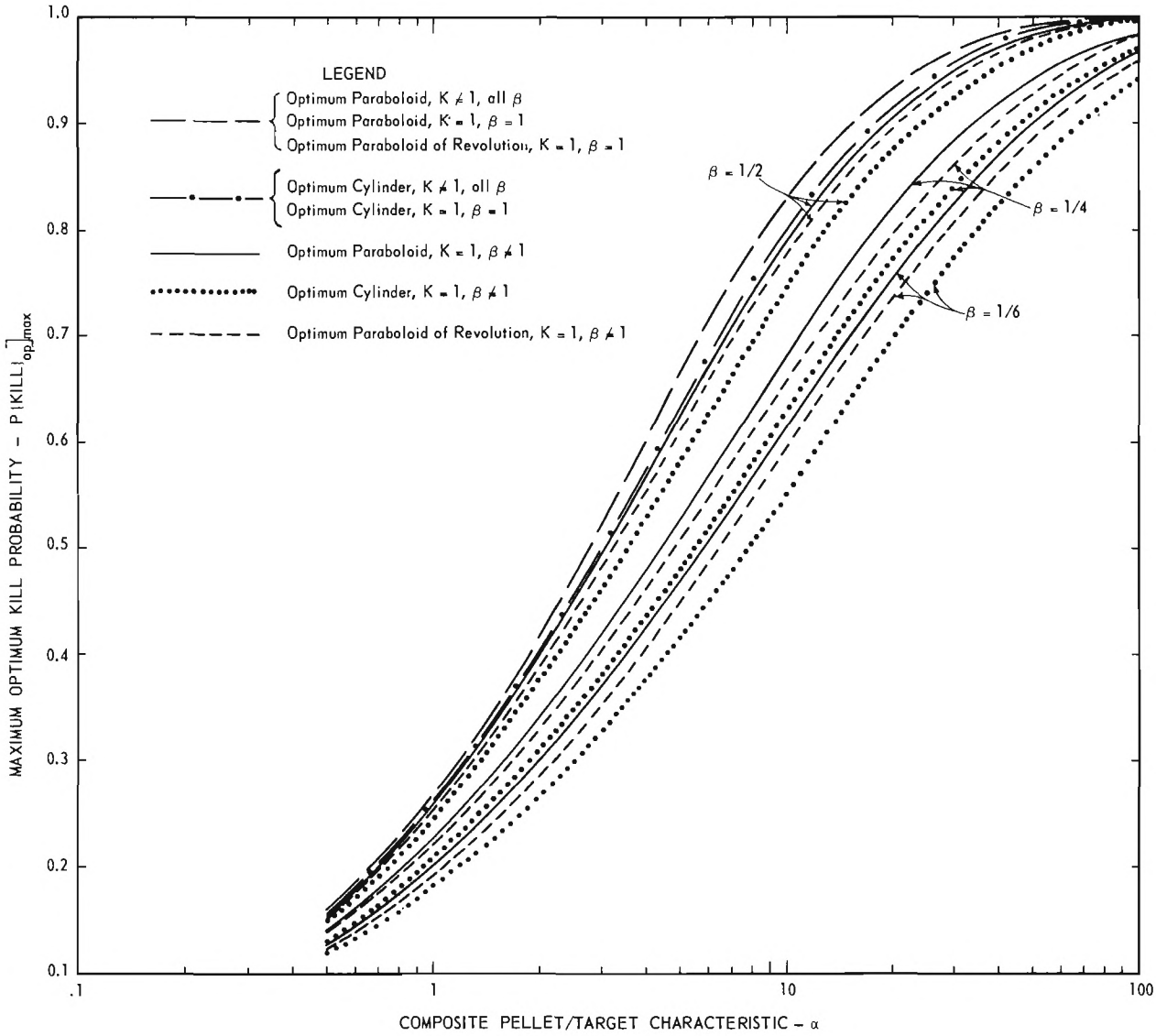

Figure 7. Maximum Kill Probability Accompanying Optimum Paraboloidal and Cylindrical Pellet Distributions Over Circular and Elliptical Laminas, for Various Values of Error-Pattern Axis Ratio β.

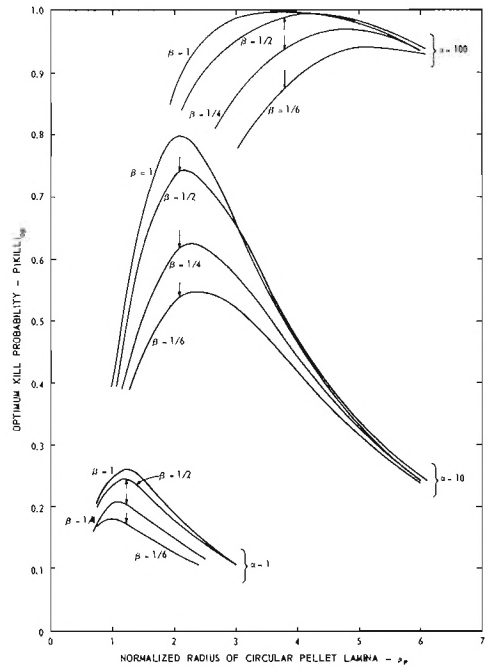

Figure 8. Kill Probability Accompanying Optimum Cylindrical Pellet Distributions over Circular Laminas, for Various Values of Error-Pattern Axis Ratio β and Composite Pellet/Target Characteristic α.

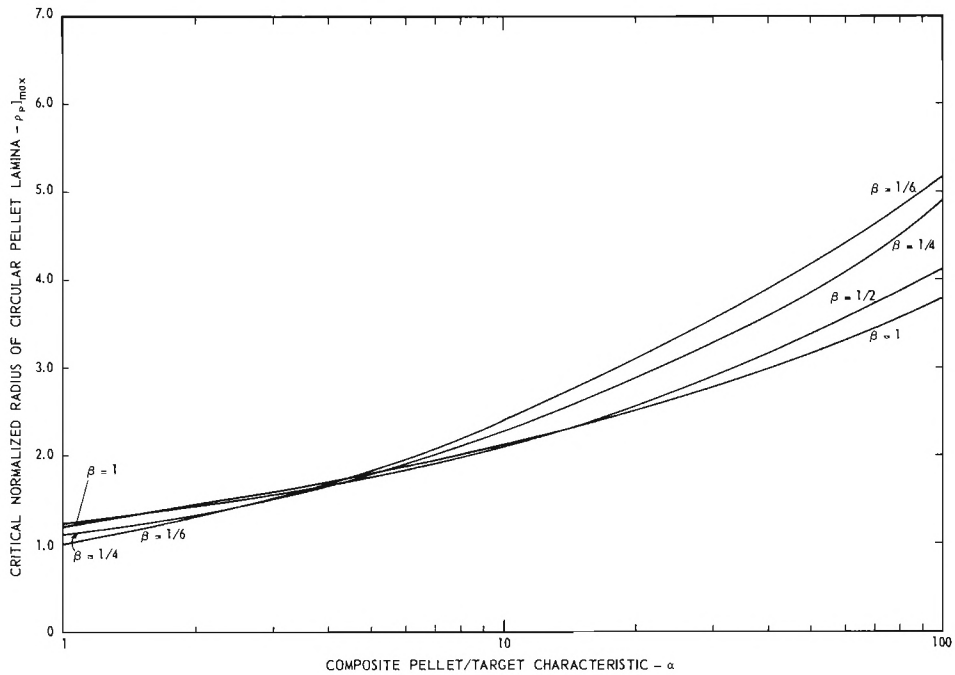

Figure 9. Normalized Radius of the Circular Pellet Lamina Which Maximizes the Kill Probability Accompanying Optimum Cylindrical Pellet Distributions, for Various Values of Error-Pattern Axis Ratio β.

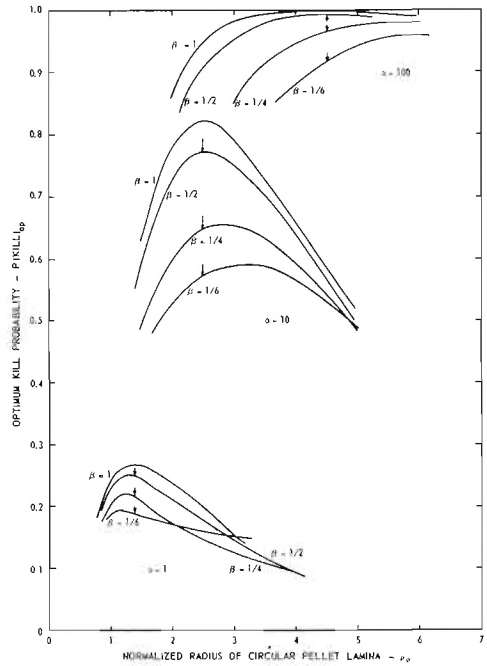

Figure 10. Kill Probability Accompanying Optimum Paraboloid-of-Revolution Pellet Distributions Over Circular Laminas, for Various Values of Error-Pattern Axis Ratio β and Composite Pellet/Target Characteristic α.

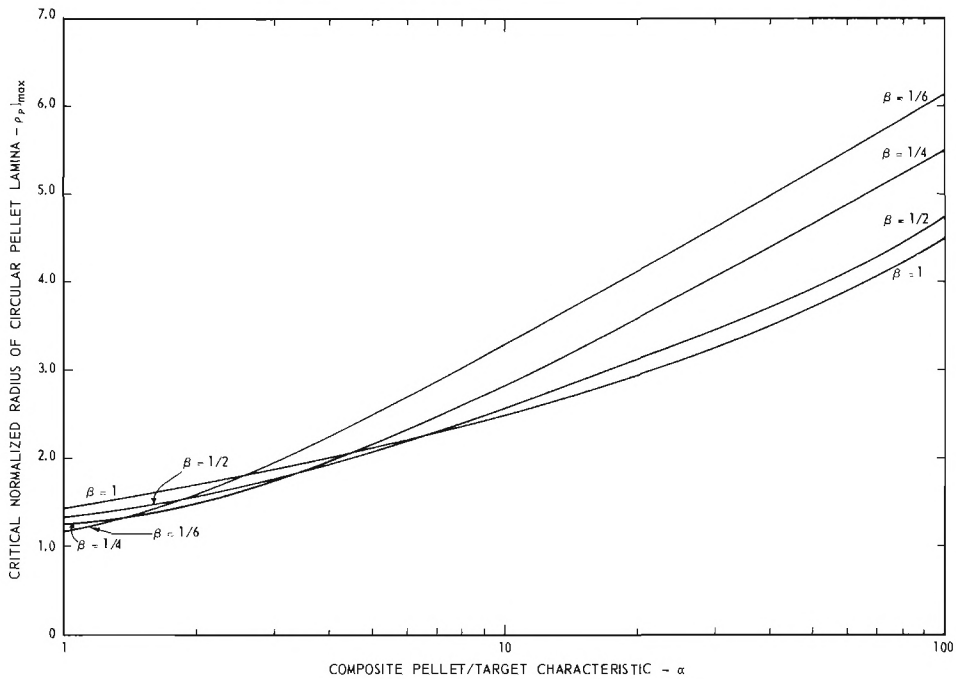

Figure 11. Normalized Radius of the Circular Pellet Lamina Which Maximizes the Kill Probability Accompanying Optimum Paraboloid-of-Revolution Pellet Distributions, for Various Values of Error-Pattern Axis Ratio β.

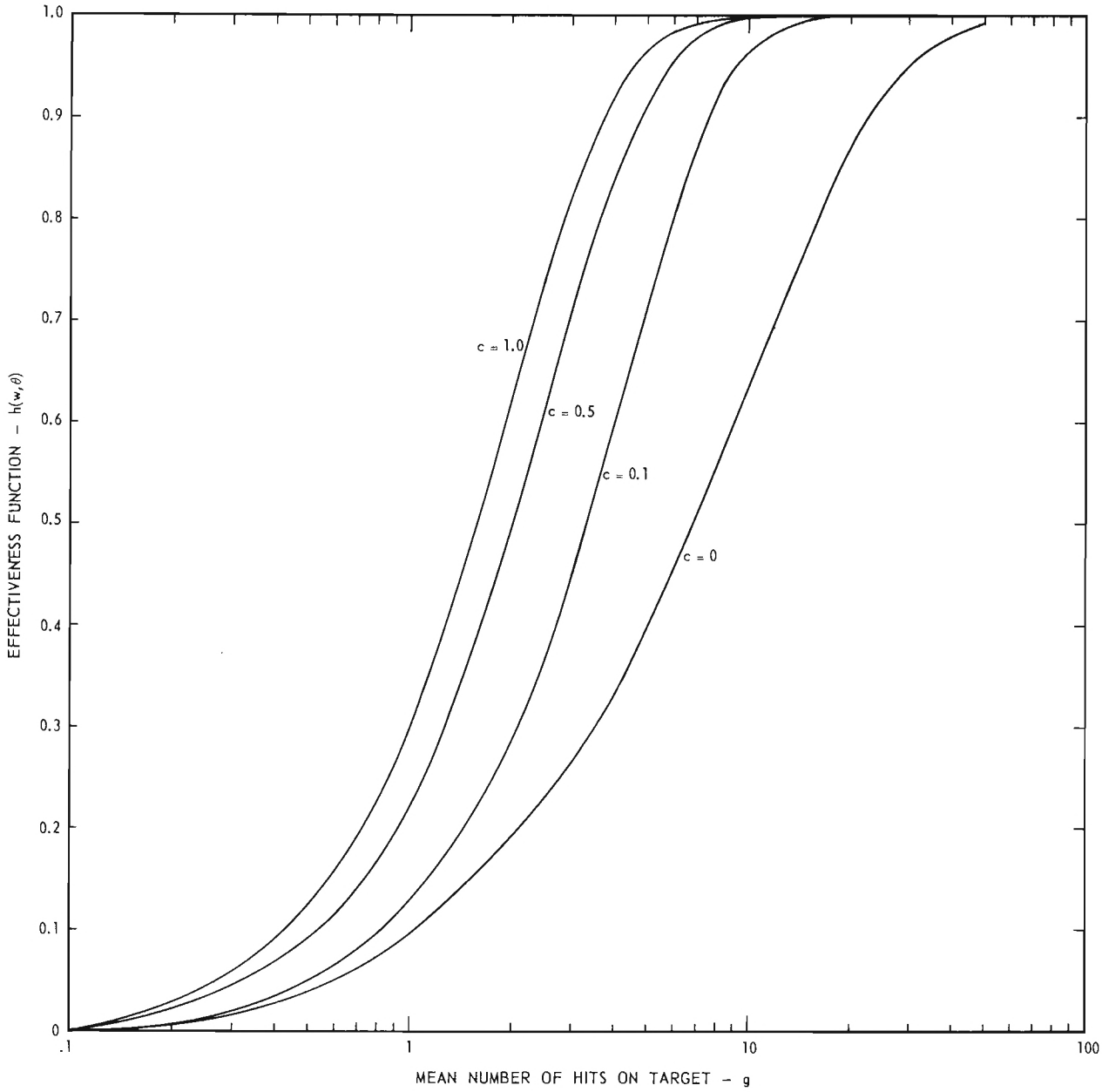

Figure 12. Effectiveness Function Accompanying Optimum Cylindrical Pellet Distributions Over Circular Laminas, for a Circular Error Pattern, Individual Pellet Kill Probability p of 0.1, and Various Values of the Tandem Pellet Factor c.

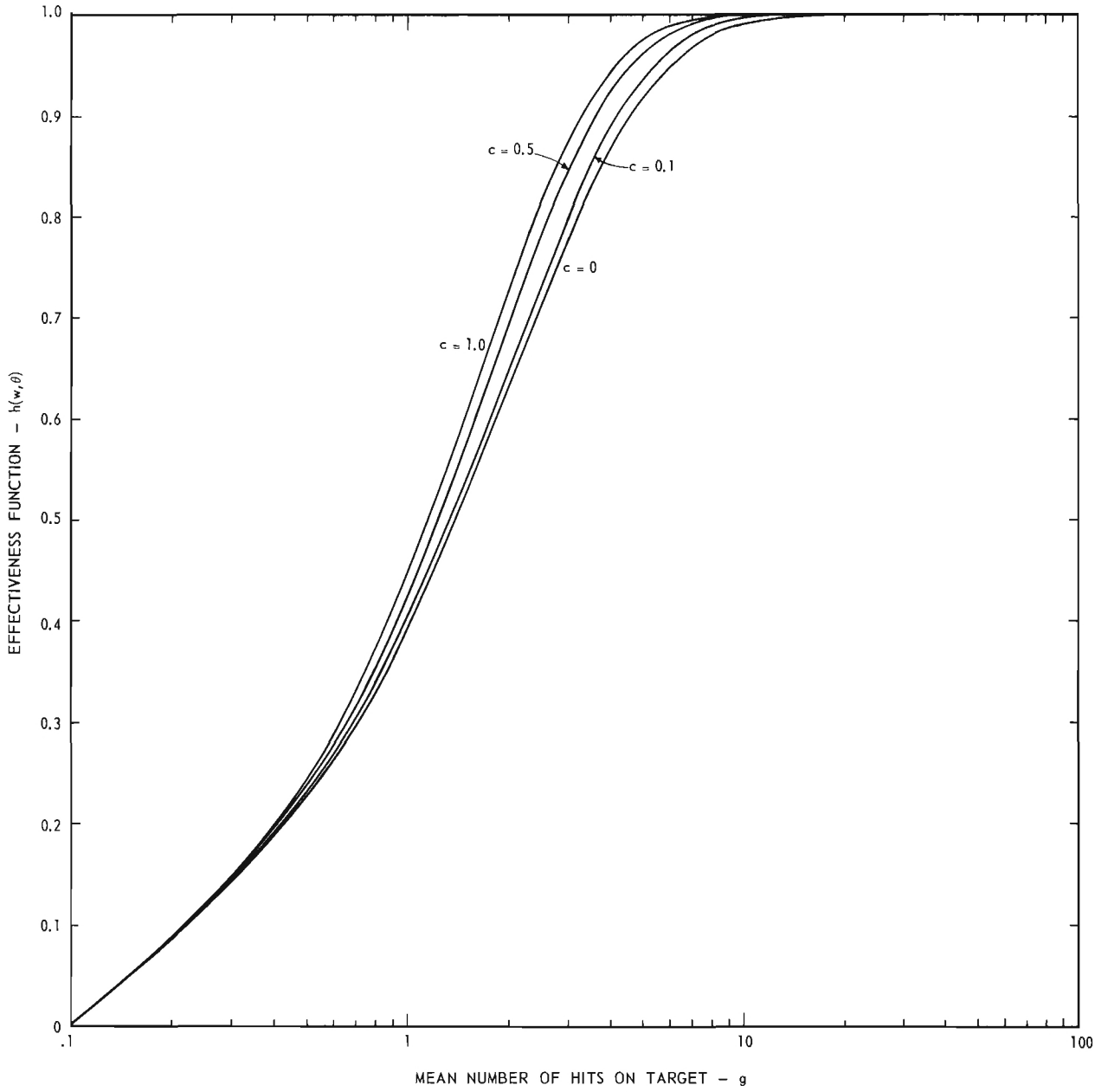

Figure 13. Effectiveness Function Accompanying Optimum Cylindrical Pellet Distributions Over Circular Laminas, for a Circular Error Pattern, Individual Pellet Kill Probability p of 0.5, and Various Values of the Tandem Pellet Factor c.

APPENDICES A AND B

APPENDIX A

DIAGONALIZATION OF THE COVARIANCE MATRIX

The covariance matrix $\overline{C}$ pertaining to the discussion of Section 2 is the following:*

$$\text{(A-1)} \qquad \overline{C} = \begin{bmatrix} \sigma_X^2 & \sigma_{XY} \\ \sigma_{XY} & \sigma_Y^2 \end{bmatrix} ,$$

where

$$\text{(A-2a)} \qquad \sigma_X^2 = \sigma_{X_T'}^2 + \sigma_{X_P'}^2 ,$$

$$\text{(A-2b)} \qquad \sigma_Y^2 = \sigma_{Y_T'}^2 + \sigma_{Y_P'}^2 ,$$

$$\text{(A-2c)} \qquad \sigma_{XY} = \sigma_{X_T'Y_T'} + \sigma_{X_P'Y_P'} ;$$

$\sigma_{X_T'}^2$, $\sigma_{Y_T'}^2$, and $\sigma_{X_T'Y_T'}$ are the variances and covariance associated with random errors in the predicted target position, while $\sigma_{X_P'}^2$, $\sigma_{Y_P'}^2$, and $\sigma_{X_P'Y_P'}$ are the variances and covariance associated with errors in the placement of the pellet pattern.

Since $\overline{C}$ is a symmetric matrix, there exists a real nonsingular linear transformation which will diagonalize it to the form [4]

$$\text{(A-3)} \qquad \overline{C}_D = \begin{bmatrix} \sigma_x^2 & 0 \\ 0 & \sigma_y^2 \end{bmatrix} ,$$

in which the diagonal elements of the transformed matrix are the characteristic roots of $\overline{C}$ found from

$$\text{(A-4)} \qquad |\overline{C} - \sigma^2 \overline{I}| = 0 .$$

*Overlining is used in this Appendix to represent vector quantities.

Upon solving the determinantal form (A-4), one finds for the diagonal elements of (A-3)

$$\text{(A-5a)} \qquad \sigma_x^2 = \frac{1}{2}\{(\sigma_X^2 + \sigma_Y^2) - [(\sigma_X^2 - \sigma_Y^2)^2 + 4\,\sigma_{XY}^2]^{\frac{1}{2}}\} \ ,$$

$$\text{(A-5b)} \qquad \sigma_y^2 = \frac{1}{2}\{(\sigma_X^2 + \sigma_Y^2) + [(\sigma_X^2 - \sigma_Y^2)^2 + 4\,\sigma_{XY}^2]^{\frac{1}{2}}\} \ ,$$

which are Equations (2b) and (2c) of the text. It is noted that $\underline{\sigma}_x^2$ has arbitrarily been chosen to be smaller than $\underline{\sigma}_y^2$; both, of course, are positive since $\overline{C}$ is positive definite.

The orthogonal transformation matrix $\overline{R}$ which diagonalizes $\overline{C}$ may be taken as the rotation matrix

$$\text{(A-6)} \qquad \overline{R} = \begin{bmatrix} \cos\varphi & \sin\varphi \\ -\sin\varphi & \cos\varphi \end{bmatrix} \ ,$$

where $\underline{\varphi}$ represents the counterclockwise angle as measured from the original X,Y coordinate system in Figure 2 to the new system x,y in which $\overline{C}$ is diagonal. Since, to diagonalize $\overline{C}$,

$$\text{(A-7)} \qquad \overline{R}'\,\overline{C}\,\overline{R} = \overline{C}_D \ ,$$

or

$$\text{(A-8)} \qquad \overline{C} = \overline{R}\,\overline{C}_D\,\overline{R}' \ ,$$

one obtains $\underline{\varphi}$ by performing the operations indicated in (A-8). Thus

$$\text{(A-9a)} \qquad \cos 2\varphi = \frac{\sigma_Y^2 - \sigma_X^2}{\sigma_y^2 - \sigma_x^2} \ ,$$

or upon introducing Equations (A-5)

$$\text{(A-9b)} \qquad \cos 2\varphi = \frac{\sigma_Y^2 - \sigma_X^2}{[(\sigma_X^2 - \sigma_Y^2)^2 + 4\,\sigma_{XY}^2]^{\frac{1}{2}}} \ .$$

APPENDIX B

REDUCTION OF AN INTEGRAL TO TABULAR FORM

Equation (40) in the text contains two double integrals of the form

$$(B\text{-}1) \qquad I(\gamma) = \int_0^{2\pi} \int_0^{\rho_P^2} \exp\left[-\gamma \frac{w}{2\beta}(\beta^2 \sin^2\theta + \cos^2\theta)\right] dw\, d\theta \quad ,$$

where γ is unity for the first integral and has the value

$$1 - \frac{8\alpha\beta}{\rho_P^4(3 - \beta^2)}$$

for the other. It is the purpose here to reduce (B-1) to the form expressed in Equation (41) and tabulated by Cox and Johnson[3].

Replacing w in (B-1) by its equivalent given in terms of r in Equation (6) and subsequently changing from polar to rectangular form, one has

$$(B\text{-}2) \qquad I(\gamma) = \frac{8}{\sigma_x \sigma_y} \int_0^{r_P} \int_0^{(r_P^2 - y^2)^{\frac{1}{2}}} \exp\left[-\frac{\gamma}{2}\left(\frac{x^2}{\sigma_x^2} + \frac{y^2}{\sigma_y^2}\right)\right] dx\, dy \quad ,$$

where β has been replaced by σ_x/σ_y as defined by Equation (4c) and ρ_P by $r_P/(\sigma_x\sigma_y)^{\frac{1}{2}}$ as given by (20). Introduction of the substitutions

$$(B\text{-}3) \qquad x = \frac{\sigma_x}{\gamma^{\frac{1}{2}}}\, s \quad ,$$

$$(B\text{-}4) \qquad y = \frac{\sigma_x}{\gamma^{\frac{1}{2}}}\, t \quad ,$$

leads to

$$(B\text{-}5) \qquad I(\gamma) = \frac{8\beta}{\gamma} \int_0^{P} \int_0^{(P^2 - t^2)^{\frac{1}{2}}} \exp\left[-\frac{1}{2}\left(s^2 + \frac{t^2}{k^2}\right)\right] ds\, dt \quad ,$$

in which

$$(B\text{-}6) \qquad k = 1/\beta \quad ,$$

$$(B\text{-}7) \qquad P = \rho_P \left(\frac{\gamma}{\beta}\right)^{\frac{1}{2}} \quad ,$$

and β and ρ_P have been reintroduced. Reference to Cox and Johnson reveals

that $\underline{I}(\gamma)$ can now be written in terms of their tabulated probability $\underline{P}_{TAB}$ (k,P):

$$(B\text{-}8) \qquad I(\gamma) = \frac{8\beta}{\gamma}\left[\frac{\pi k}{2} P_{TAB}(k,P)\right] ,$$

$$= \frac{4\pi}{\gamma} P_{TAB}(k,P) \quad .$$

In evaluating the first of the double integrals in Equation (40), $\underline{\gamma}$ has the value unity and $\underline{P}$ takes the special form $\underline{A}_P$:

$$(B\text{-}9) \qquad A_P = \rho_P/\beta^{\frac{1}{2}} \quad .$$

Then

$$(B\text{-}10) \qquad I(1) = 4\pi P_{TAB}(k,A_P) \quad .$$

For the second double integral in (40), $\underline{\gamma}$ has the form cited earlier and the corresponding value of $\underline{P}$ is designated as $\underline{B}_P$ which with the aid of (B-9) becomes

$$(B\text{-}11) \qquad B_P = A_P\left[1 - \frac{8\alpha}{\beta(3 - \beta^2)A_P^4}\right]^{\frac{1}{2}} \quad .$$

In this case Equation (B-8) is written

$$(B\text{-}12) \qquad I\left(1 - \frac{8\alpha\beta}{\rho_P^4(3 - \beta^2)}\right) = 4\pi \left(\frac{A_P}{B_P}\right)^2 P_{TAB}(k,B_P) \quad .$$

Equations (B-10) and (B-12) together yield Equation (41) of the text.

REFERENCES

1. A. Grad and H. Solomon, "Distribution of Quadratic Forms and Some Applications," The Annals of Mathematical Statistics, Vol. 26, No. 3, September 1955.

2. P. M. Morse and G. E. Kimball, Methods of Operations Research, The Technology Press of Massachusetts Institute of Technology and John Wiley and Sons, Inc., New York, 1950.

3. P. C. Cox and C. Johnson, "Tables for Computing Radial Probability," Ordnance Mission, White Sands Proving Ground, New Mexico, Technical Memorandum No. 491, January 1958.

4. T. N. Anderson, An Introduction to Multivariate Statistical Analysis, John Wiley and Sons, Inc., New York, 1958.